Original Article

Institution of MECHANICAL ENGINEERS
Journal of AUTOMOBILE ENGINEERING

Proc IMechE Part D:
J Automobile Engineering
227(12) 1636–1649

DOI: 10.1177/0954407013502319
pid.sagepub.com
SAGE

Active front-steering control of a sport utility vehicle using a robust linear quadratic regulator method, with emphasis on the roll dynamics

Naser Elmi[1], Abdolreza Ohadi[1] and Behzad Samadi[2]

Abstract

One of the well-known methods for improving the lateral stability of a vehicle is to utilize an active steering controller. Common active steering systems use feedback signals from a yaw rate sensor and side-slip angle estimation. However, in some driving conditions, skilled drivers can prevent vehicle rollover using the steering angle of the vehicle. Hence, the effect of an active front-steering controller on the roll angle of the vehicle is studied in this paper. For this study, a three-degree-of-freedom linear model of a vehicle which has the lateral motion, the yaw motion and the roll motion as the degrees of freedom is derived. The effectiveness of the active steering controller on the roll stability of the vehicle is examined by simulations in a wide range of longitudinal velocities of the vehicle using a linear quadratic regulator controller. The results obtained indicate that the active steering controller increases the roll stability of the vehicle only at low vehicle speeds and also that consideration of the roll degree of freedom in the design of the active steering controller is not effective at high vehicle speeds. Therefore a two-degree-of-freedom bicycle model is sufficient for active steering controller design. Another part of this paper is dedicated to designing a practical active steering controller for a vehicle with time-varying and uncertain parameters. In fact, designing a controller which guarantees the stability of the vehicle with simultaneous uncertainties in the cornering stiffnesses of the tyres and in the time-varying velocity is the main goal of this paper. Another important advantage of the proposed controller is its simplicity and static structure. In fact, this controller design is carried out offline and can be implemented for use in a real vehicle. This simple and powerful controller is a robust linear quadratic regulator controller. For designing a robust linear quadratic regulator controller, a polytopic model of the two-degree-of-freedom vehicle is obtained, which considers the uncertainty in the parameters. In addition, a linear matrix inequality is used to design a linear quadratic regulator controller for an uncertain or parameter-varying system. Finally, the performance of the designed robust linear quadratic regulator controller was studied by simulating the vehicle responses in some manoeuvres. A sport utility vehicle model is used for simulation purposes. This non-linear vehicle model has eight degrees of freedom and its tyres are assumed to be both linear and non-linear. The performance of the robust linear quadratic regulator controller was studied for vehicles with both linear and non-linear Pacejka tyres. The proposed controller guarantees robust stability of the closed-loop system in the presence of 50% variation in the vehicle speed and 20% uncertainty in the stiffnesses of the tyres.

Keywords

Active front steering, lateral stability, roll stability, polytopic, robust linear quadratic regulator, linear matrix inequality

Date received: 25 October 2012; accepted: 29 July 2013

Introduction

The rollover and lateral instability of vehicles cause a meaningful percentage of fatalities in all the road accident modes. One of the categories in vehicle rollover is on-road rollover which is produced as a result of violent manoeuvres. This type of rollover is generally called yaw-induced rollover. In the last two decades, the usage of sport utility vehicles (SUVs) has progressively increased and so the lateral stability and roll

[1]Department of Mechanical Engineering, Amirkabir University of Technology (Tehran Polytechnic), Tehran, Iran
[2]Department of Electrical Engineering, Amirkabir University of Technology (Tehran Polytechnic), Tehran, Iran

Corresponding author:
Abdolreza Ohadi, Department of Mechanical Engineering, Amirkabir University of Technology (Tehran Polytechnic), 424 Hafez Avenue, Tehran, Iran.
Email: a_r_ohadi@aut.ac.ir

stability of these types of vehicle have attracted more attention. As mentioned in the literature, there are four different methods for controlling the roll stability of a vehicle and these methods are categorized on the basis of their actuators: active steering, active anti-roll bar, active suspension and active differential braking. An active steering system[1] and differential braking[2,3] control the yaw moment and the lateral stability of a vehicle. These systems can be used to improve the roll stability of a vehicle in some conditions. However, not many studies have been performed on the application of indirect roll control methods. To the best of our knowledge, the investigation which has been carried out by Shim et al.[4] is the only work which studied the effect of an active steering system in rollover recovery. In that study, combined active steering and a differential braking system were used to control the tripped rollover of a vehicle without considering the lateral stability. Indeed, in that work a 14-degree-of-freedom vehicle model and a model-free proportional–integral–derivative (PID) controller for recovering the roll instability were used. However, that article indicated that a steering system is effective for only low-speed rollovers.

In the present work a three-degree-of-freedom (3DOF) linear vehicle model is used to study the importance of roll dynamics in active steering controller design. Using this model we investigated whether an active steering controller can improve the roll stability.

This 3DOF model has the roll motion, the yaw motion and the lateral motion as the degrees of freedom and is used in linear quadratic regulator (LQR) controller design. The results of this study compare the performance when using the 3DOF linear model with that when using the two-degree-of-freedom (2DOF) bicycle model in active steering controller design.

As mentioned, the main goal of the active steering controller is to improve the lateral stability and the directional stability of the vehicle. Many methods of controller design have been used for designing an active steering controller. For example a model predictive controller based on a 2DOF non-linear model of the vehicle was designed and implemented on a Ford automobile by Falcone et al.[5] Furthermore, quantitative feedback theory (QFT) was used for designing an active front steering controller.[6] Another method, which is used in this category, is feedback linearization. Hsu and Gerdes[7] designed this controller on the basis of a 2DOF non-linear vehicle model. A gain-scheduled robust controller for a parameter-varying vehicle which has integrated active steering and a differential braking system has been designed by Baslamisli et al.[8] Also, a driver steering assistance controller system for lane departure avoidance was designed by Minoiu Enache et al.[9] using a linear matrix inequality (LMI) and a Lyapunov function for time-varying adhesion and velocity conditions. The steering assistance system aims to avoid unintended lane departure during normal driving; in that work a linear state feedback controller was used for this purpose, based on a bicycle vehicle model. Moreover, Goodarzi et al.[10] used fuzzy controllers to design an active steering system. Also, the independence of the front wheels was considered in their study.

The other and major contribution of this work is to design a novel active steering controller which has the advantages of both simplicity and robustness simultaneously. Because of the many sources of uncertainty such as the variable vehicle speed and the parameter-dependent cornering stiffnesses of the tyres, the active steering controller should be robust with respect to these uncertainties and time-varying parameters. Furthermore, an LQR controller is a well-known controller that is designed and implemented simply. If an LQR controller with a constant gain is designed for all the possible uncertain parameters of vehicle, then the resulting controller will be a robust LQR controller. The LMI can be used to express the problem when the dynamics of the system are polytopic. The main goal of this study is to represent the uncertain dynamics of the vehicle in polytopic form and to design a robust LQR controller for a vehicle which has uncertainties in the cornering stiffnesses of the tyres and the vehicle speed simultaneously. The robust LQR controller is a novel idea in the lateral stability control of a vehicle but has been used in controlling pulse-width-modulated (PWM) converters[11] and in voltage control of wind farms[12] in recent years. In PWM converters, the system dynamics change using a switch and, in wind farms, the system dynamics are a function of the parameters; therefore, the system dynamics in both cases are parameter dependent.

The remaining sections of this paper are organized as follows: in the second section, the vehicle models for simulation purposes and controller design are derived. In the third section, the roll dynamics and the advantages in active steering controller design are studied; consequently, in the fourth section, the controller design problem using an LMI representation is given, and also the polytopic modelling of the 2DOF vehicle is presented in this section. The fifth section presents design example results for a vehicle with a harmonic steering input and a constant longitudinal velocity. Finally, the conclusions of the paper are presented in the sixth section.

Vehicle models

In this section, three different vehicle models are presented for different purposes: the first model is the eight-degree-of-freedom (8DOF) non-linear vehicle model which is used for simulation purposes; the second model is the 3DOF linear vehicle model which is applied for the first time for considering the effect of the roll dynamics in active steering controller design; the third model is the common 2DOF linear model for controller design.

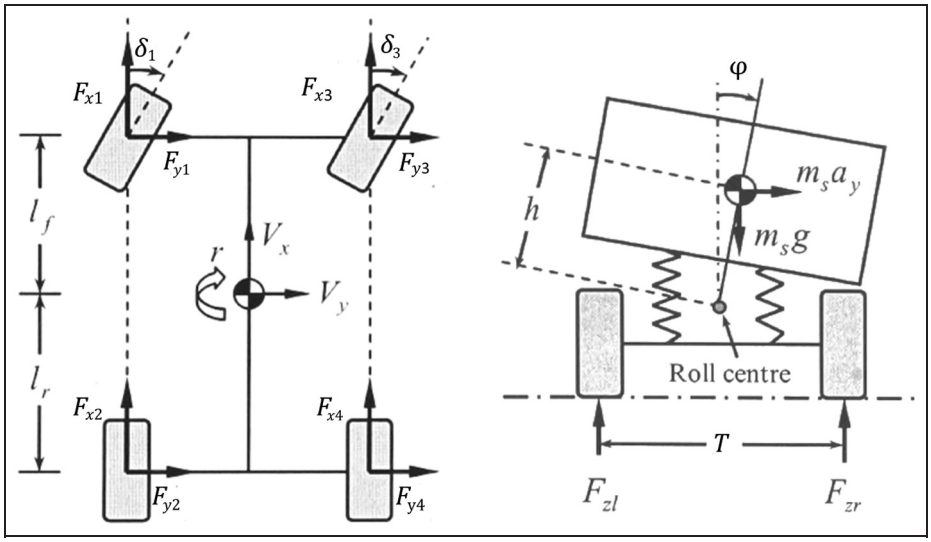

Figure 1. Degrees of freedom and coordinate system of the vehicle.[13]

Non-linear eight-degree-of-freedom vehicle model

This 8DOF vehicle model is used for simulation purposes and includes three planar motions of a vehicle chassis (the longitudinal motion, the lateral motion and the yaw motion) and also a degree of freedom for the sprung-mass roll motion about its roll axis and four degrees of freedom for the rotation of each wheel. Generally, in the handling analysis it is assumed that there is no hard braking and accelerating and that the vehicle moves on a smooth flat road; therefore, the body pitch and vertical motions of the vehicle are ignored. Furthermore, the dynamics of the steering actuator, the driving actuator and the braking actuator are neglected for simplicity.

Figure 1 indicates the vehicle model, its coordinate system, the degrees of freedom and also the external forces. The equations of motion for this model are defined as[13]

$$m(\dot{V}_x - V_y r) - m_s h \dot{r}\varphi = \sum F_x \tag{1}$$

$$m(\dot{V}_y + V_x r) + m_s h \ddot{\varphi} = \sum F_y \tag{2}$$

$$I_{zz}\dot{r} - I_{xz}\ddot{\varphi} = \sum M_z \tag{3}$$

$$I_{xx}\ddot{\varphi} + m_s h(\dot{V}_y + V_x r) - I_{xz}\dot{r} = \sum M_x \tag{4}$$

$$I_w \dot{\omega}_i = -R_w F_{xwi} + T_i, \quad i = 1, \ldots, 4 \tag{5}$$

where V_x, V_y, r, φ and ω_i are the longitudinal velocity, the lateral velocity, the yaw rate, the roll angle and the angular velocity of the ith wheel respectively; also m, m_s, I_{zz}, I_{xx}, I_{xz}, I_w, R_w and T_i are the total mass, the sprung mass, the moment of inertia about the yaw axis, the sprung-mass moment of inertia about the roll axis, the sprung-mass product of the inertia about the roll and yaw axes, the moment of inertia of the wheel, the radius of the wheel and the braking torque on each wheel respectively. The other terms are the total forces and moments which are exerted on the vehicle in the centre-of-mass coordinate system and are defined as

$$\sum F_x = F_{x1} + F_{x2} + F_{x3} + F_{x4} \tag{6}$$

$$\sum F_y = F_{y1} + F_{y2} + F_{y3} + F_{y4} \tag{7}$$

$$\sum M_z = L_f(F_{y1} + F_{y2}) - L_r(F_{y3} + F_{y4}) \tag{8}$$

$$\sum M_x = [m_s g h - (K_{\varphi f} + K_{\varphi r})]\varphi - (C_{\varphi f} + C_{\varphi r})\varphi \tag{9}$$

$$m = m_s + m_{uf} + m_{ur} \tag{10}$$

where h, $K_{\varphi f}$ and $K_{\varphi r}$ are the distance from the sprung-mass centre of gravity to the roll axis, the front-suspension roll stiffness and the rear-suspension roll stiffness respectively. Also $C_{\varphi f}$ and $C_{\varphi r}$ are the front-suspension damping coefficient and the rear-suspension damping coefficient respectively. In the presented equations, the longitudinal and lateral forces of the tyres along the wheel axes should be presented in the vehicle's fixed-coordinate system. The equations which translate the force axes of the ith wheel to the global fixed axes are given by

$$\begin{Bmatrix} F_{xi} \\ F_{yi} \end{Bmatrix} = \begin{bmatrix} \cos\delta_i & -\sin\delta_i \\ \sin\delta_i & \cos\delta_i \end{bmatrix} \begin{Bmatrix} F_{xwi} \\ F_{ywi} \end{Bmatrix}, \quad i = 1, \ldots, 4 \tag{11}$$

In the above equation, F_{xi} and $F_{yi}$are the forces generated by the ith wheel, which are presented in the global coordinate system. Furthermore, F_{xwi}, F_{ywi} and δ_i are the longitudinal force, the lateral force and the steering angle respectively generated by the ith wheel.

In this study it is assumed that the front wheels of the vehicle can be steered and that the steering angles of the rear wheels are zero; therefore, the steering angle of each wheel has the relations

$$\delta_1 = \delta_2 = \delta, \quad \delta_3 = \delta_4 = 0 \tag{12}$$

The side-slip angle for each wheel can be defined as

$$\begin{aligned}\alpha_1 &= \arctan\left(\frac{V_y + L_f r}{V_x + Tr/2}\right) - \delta \\ \alpha_2 &= \arctan\left(\frac{V_y - L_r r}{V_x + Tr/2}\right) \\ \alpha_3 &= \arctan\left(\frac{V_y + L_f r}{V_x - Tr/2}\right) - \delta \\ \alpha_4 &= \arctan\left(\frac{V_y - L_r r}{V_x - Tr/2}\right)\end{aligned} \tag{13}$$

Also, the side-slip angle β of the vehicle is defined as

$$\beta \approx \frac{V_y}{V_x} \tag{14}$$

The linear tyre model is used in the major part of this study. However, in a few cases a non-linear Pacejka model is used. This model depends on the side-slip angle of each wheel. However, the cornering stiffness depends on the tyre pressure, the normal force on tyre and the coefficient of friction in the real world, and so there is uncertainty in the cornering stiffnesses of the tyres. The equation of the lateral force of a linear tyre is given by

$$F_{ywi} = C_{\alpha_i}\alpha_i, \quad i = 1, \ldots, 4 \tag{15}$$

with

$$\begin{aligned}C_{\alpha f} &= C_{\alpha_1} + C_{\alpha_3} \\ C_{\alpha r} &= C_{\alpha_2} + C_{\alpha_4}\end{aligned}$$

The reference model is used to calculate the desired yaw rate, which should be generated by the active steering system. The goal of the active steering controller is to track the desired yaw rate signal and to guarantee the stability of the side-slip angle. In fact, the driver's steering input is changed to the desired yaw rate, which is dependent on the longitudinal velocity V_x of the vehicle, the coefficient μ of friction of the road, the steering input δ of the driver and the vehicle parameters such as the mass m, the lateral stiffness $C_{\alpha f}$ of the front tyres, the lateral stiffness $C_{\alpha r}$ of the rear tyres, the distance L_f from the centre of gravity to the front axle and the distance L_r from the centre of gravity to the rear axle. This model was derived on the basis of steady-state steering on a circular path. The equation of reference model has been defined as[14]

$$\begin{aligned}r_{ref} &= \frac{V_x}{(L_f + L_r) + mV_x^2(L_r C_{\alpha r} - L_f C_{\alpha f})/2C_{\alpha r}C_{\alpha f}(L_f + L_r)}\delta \\ r_{upperbound} &= 0.85\frac{\mu g}{V_x} \\ r_d &= \begin{cases} r_{ref}, & |r_{ref}| \leqslant r_{upper\ bound} \\ r_{upper\ bound}\ \mathrm{sgn}(r_{upper\ bound}), & |r_{ref}| > r_{upper\ bound} \end{cases} \\ \beta_d &\approx 0\end{aligned} \tag{16}$$

The goal of the active steering controller is to track the reference signals in equation (16), and the performance of designed controller is analysed on the basis of this reference model.

Three-degree-of-freedom linear vehicle model

As mentioned before, the purposes of the active steering controller are to track the desired yaw rate and also to regulate the side-slip and the roll motion. In this regard, we considered in our study the effect of the coupling terms between the roll motion and the lateral motion in controller design. In addition, the performance of the active steering controller as an anti-roll system is investigated here. For this study a 3DOF linear model of vehicle is derived. The degrees of freedom of this model are the lateral velocity, the yaw rate and the roll angle. Therefore, the model has the ability to illustrate the coupling effects between the lateral motion and roll motion of the vehicle and the performance of the active steering controller as an anti-roll system. As mentioned before, there have not been many studies about the effect of active steering control on the roll dynamics and the effect of the roll dynamics in designing active steering controllers. Hence, in this study, the 3DOF linear model of a vehicle is used in active steering controller design.

For deriving the dynamics of the 3DOF vehicle model, it is assumed that the effect of the unsprung masses can be neglected. Using the Newton–Euler method, the dynamic equations for this model are given by

$$\begin{aligned}\sum_{i=1}^{4} F_{yi} &= m\dot{V}_y - m_s h\ddot{\varphi} + mrV_x \\ \sum M_z &= I_{zz}\dot{r} \\ \sum M_{xs} &= I_{xxs}\ddot{\varphi} - m_s h(\dot{V}_y - h\ddot{\varphi} + rV_x)\end{aligned} \tag{17}$$

By assuming that $|V_x| \gg |Tr|$ in equation (13), the side-slip angle of each wheel can be expressed as

$$\begin{aligned}\alpha_1 = \alpha_3 &= \beta + \frac{L_f}{V_x}r - \delta \\ \alpha_2 = \alpha_4 &= \beta - \frac{L_r}{V_x}r\end{aligned} \tag{18}$$

With replacement of the forces and the moments due to interaction of the tyres with the road in the linear range, the 3DOF linear dynamic model of a vehicle is expressed as

$$\begin{bmatrix}\dot{\beta} \\ \dot{r} \\ \dot{\varphi} \\ \ddot{\varphi}\end{bmatrix} = \begin{bmatrix}\frac{G_{11}}{V_x} & \frac{G_{12}}{V_x} & \frac{G_{13}}{V_x} & \frac{G_{14}}{V_x} \\ G_{21} & G_{22} & 0 & 0 \\ 0 & 0 & 0 & 1 \\ G_{41} & G_{42} & G_{43} & G_{44}\end{bmatrix}\begin{bmatrix}\beta \\ r \\ \varphi \\ \dot{\varphi}\end{bmatrix} + \begin{bmatrix}\frac{A_{11}C_{\alpha f}}{V_x} \\ \frac{L_f C_{\alpha f}}{I_{zz}} \\ 0 \\ B_{12}C_{\alpha f}\end{bmatrix}\delta \tag{19}$$

In equation (19) the dynamic matrix elements G_{ij} are defined in Appendix 1.

Two-degree-of-freedom linear vehicle model (bicycle model)

Another vehicle model which is used in active steering controller design is the common 2DOF linear model. This model does not consider the effect of roll dynamics in designing an active steering controller. Therefore the results of the controller designed on the basis of this model can be compared with the corresponding results of the 3DOF linear vehicle model presented in the above section. The governing equations of this model are presented as[15]

$$\begin{bmatrix}\dot{\beta}\\ \dot{r}\end{bmatrix} = \begin{bmatrix} f_{11} & f_{12}\\ f_{21} & f_{22}\end{bmatrix}\begin{bmatrix}\beta\\ r\end{bmatrix} + \begin{bmatrix}\frac{C_{\alpha f}}{mV_x}\\ \frac{L_f C_{\alpha f}}{m}\end{bmatrix}\delta$$
$$f_{11} = -\frac{C_{\alpha_1}+C_{\alpha_2}+C_{\alpha_3}+C_{\alpha_4}}{mV_x}$$
$$f_{12} = \frac{-C_{\alpha_1}L_f - C_{\alpha_3}L_f + C_{\alpha_2}L_r + C_{\alpha_4}L_r}{mV_x^2} - 1 \qquad (20)$$
$$f_{21} = \frac{-L_f C_{\alpha_1} - L_f C_{\alpha_3} + L_r C_{\alpha_2} + L_r C_{\alpha_4}}{I_{zz}}$$
$$f_{22} = -\frac{L_f^2 C_{\alpha_1} + L_f^2 C_{\alpha_3} + L_r^2 C_{\alpha_2} + L_r^2 C_{\alpha_4}}{I_{zz}V_x}$$

In the next section, the effect of considering the roll dynamics in designing an active steering controller and the conditions by which the controller improves the roll stability are studied via simulations. The well-known LQR controller is used in all the studies.

Roll dynamics effects

In this section the coupling effect of the roll dynamics and the lateral dynamics of the vehicle and also the effect of the active steering system in improving the roll stability are studied. For this purpose, two different vehicle models for controller design are considered. In the first model, the active steering controller is designed on the basis of the 2DOF vehicle model (see the section on the 2DOF linear vehicle model (bicycle model)); therefore, the coupling effect of the roll dynamics and the lateral dynamics is ignored and also the roll stability does not play a role in controller design. In the second model, the active steering controller is designed on the basis of a 3DOF vehicle model (see the section on the 3DOF linear vehicle model). The LQR controllers based on the 2DOF model and the 3DOF model are designed for oversteer and understeer vehicles by considering the effect of the vehicle speed. The designed LQR controllers are implemented using the 8DOF nonlinear simulation model of an SUV (see Appendix 2). In this section, two different manoeuvres are used to study the performances of the controllers. The first manoeuvre consists of a harmonic steering input with an amplitude of 10° and a frequency of 5 rad/s. Also the second manoeuvre is the well-known J-turn test designed by the National Highway Transport Safety Administration (NHTSA).[16]

Note that the LQR controller is selected for this purpose because this controller is the simplest model-based controller which can illustrate the effect of considering the roll motion in active steering controller design. The weight matrix Q of the states in this section is designed on the basis of two different ideas. In the first design, our main purpose is the lateral stability of vehicle but the roll stability has just as much importance as the yaw rate; therefore, the roll angle and the yaw rate of the weight matrix have the same weights. In the second case, the roll stability is more important and so has a greater weight. By a trial-and-error procedure the weight matrix of the 3DOF LQR controller in the first case was designed as $Q = \mathrm{diag}(100, 500, 500, 1)$. In the second case the roll stability is very important; therefore, its weight is increased 20 times, and the weight matrix is selected as $Q = \mathrm{diag}(100, 500, 10,000, 1)$. Finally, the weight matrix for the 2DOF controller is $Q = \mathrm{diag}(100, 500)$.

In the first part of this section, the performances of these LQR controllers are studied using the harmonic steering input. The performances of the controllers for understeer and oversteer vehicles at different velocities are studied, and the steady-state maximum values of the outputs are presented in the following tables. In Table 1 and Table 2 the controller weight matrix has equal weights for the roll angle and the yaw rate. Note that the understeer gradients of the vehicle for Table 1 and Table 2 have the same magnitudes but different signs; in fact, only the stiffnesses of the tyres and the location of the centre of mass are reversed. Note that, with the parameters in Table 4 in Appendix 2, an oversteer vehicle is considered. In Table 3 a controller with a

Table 1. Oversteer vehicle with $Q = \mathrm{diag}(100, 500, 500, 1)$ with a steering input of $0.1745\sin(5t)$.

V(m/s)	LQR 2DOF model			LQR 3DOF model		
	e_r (rad/s)	β (rad)	φ (deg)	e_r (rad/s)	β (rad)	φ (deg)
10	0.071	0.070	11.08	0.096	0.068	10.77
20	0.033	0.079	9.55	0.044	0.079	9.37
30	0.023	0.093	8.79	0.035	0.094	8.79

LQR: linear quadratic regulator; 2DOF: two-degree-of-freedom; 3DOF: three-degree-of-freedom.

Table 2. Understeer vehicle with Q = diag(100, 500, 500, 1) with a steering input of 0.1745 sin(5t).

V(m/s)	LQR 2DOF model			LQR 3DOF model		
	e_r (rad/s)	β (rad)	φ (deg)	e_r (rad/s)	β (rad)	φ (deg)
10	0.051	0.065	4.27	0.056	0.068	4.24
20	0.035	0.090	8.81	0.047	0.090	8.35
30	0.026	0.101	13.32	0.034	0.100	13.17

LQR: linear quadratic regulator; 2DOF: two-degree-of-freedom; 3DOF: three-degree-of-freedom.

Table 3. Oversteer vehicle with Q = diag(100, 500, 10,000, 1) with a steering input of 0.1745 sin(5t).

V(m/s)	LQR 2DOF model			LQR 3DOF model		
	e_r (rad/s)	β (rad)	φ (deg)	e_r (rad/s)	β (rad)	φ (deg)
10	0.071	0.070	11.08	0.385	0.047	7.04
30	0.023	0.093	8.79	0.042	0.092	8.67

LQR: linear quadratic regulator; 2DOF: two-degree-of-freedom; 3DOF: three-degree-of-freedom.

roll stability which has a greater weight is used at two different speeds.

Table 1 indicates the variations in the yaw rate tracking error e_r (rad/s), the side-slip angle β (rad) and the roll angle φ (deg) versus the vehicle speed. Also, in this table, a comparison between the performances of the two controllers which are designed on the basis of the 2DOF and 3DOF models are presented. With reference to this table, it is obvious that an active steering controller, which is designed on the basis of the 3DOF model, has slightly more improvement in controlling the roll angle at low speeds, but at $V = 30$ m/s they are the same. Also, the yaw rate tracking errors for the 2DOF and 3DOF controllers indicate that the 2DOF controller has less tracking error in all the conditions. This result is predictable because both controllers have the same weights for the yaw rate and the side-slip but the 3DOF controller has two more states, namely the roll angle and the roll rate. Moreover, the yaw rate tracking errors for both the controllers are very small; note that the magnitude of the desired yaw rate is 1 rad/s.

Table 2 indicates the same result for the understeer vehicle, as seen also in Table 1 and Table 2; i.e. it is obvious that the roll angle for the understeer vehicle is smaller than for the oversteer vehicle. Finally, Table 3 indicates that the active steering controller performance with more importance on the roll stability is effective only at low speeds such as $V = 10$ m/s. At high velocities, the results for the 3DOF controller and the 2DOF controller are very close. Moreover, at low speeds such as $V = 10$ m/s, the yaw rate tracking error is very poor. Considering all these results, an active steering controller is not very effective in roll control; also the 2DOF vehicle model for controller design seems to be sufficient.

The second test is the J-turn manoeuvre on an oversteer vehicle at a velocity of 30 m/s. Figure 2 displays the steering angle for an open-loop system and a closed-loop system. Figure 3, Figure 4 and Figure 5 show the yaw rate signal, the side-slip angle and the roll angle respectively.

Figure 2 displays the input signal shape for a J-turn test; also the closed-loop input signals indicate the oversteer nature of vehicle, because closed-loop signals are larger than open-loop signals in the constant part of the input. Figure 3 shows that the best tracking performance belongs to the LQR controller based on the 2DOF vehicle model. Also, Figure 5 indicates that the LQR controller based on the 2DOF model and the LQR controller based on the 3DOF model do not have a significant difference in regulating the roll angle. Finally, Figure 4 indicates the side-slip angle stability of the designed controllers and insignificant difference between the two controllers. Considering all this, it is reasonable to use the 2DOF model of a vehicle in active steering controller design. Although an active steering controller may be useful at very low speeds to control the roll angle, the main application of an active steering system is at high speeds. These results agree with the results obtained by Shim et al.[4]

As a summary, an active steering controller is not able to control the vehicle rollover or the roll stability at high longitudinal velocities, and this controller should be used for roll stability control only at low speeds. Also the results of this study show that in a wide range of velocities the effect of the roll dynamics on active steering controller design is negligible and that the 2DOF bicycle model is sufficient for this purpose. These results expand the results obtained by Shim et al.[4] who used a model-free PID controller for improving the roll stability by an active steering controller.

Because of the results obtained in this section, in the next section a 2DOF vehicle model is used to design an LQR active steering controller.

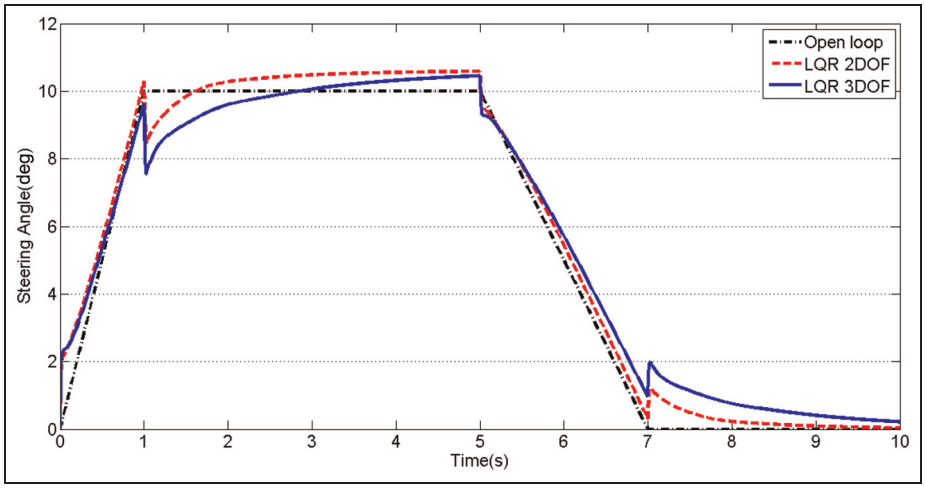

Figure 2. Steering angle (input signal) for a J-turn test with V = 30 m/s for various models.
LQR: linear quadratic regulator; 2DOF: two-degree-of-freedom; 3DOF: three-degree-of-freedom.

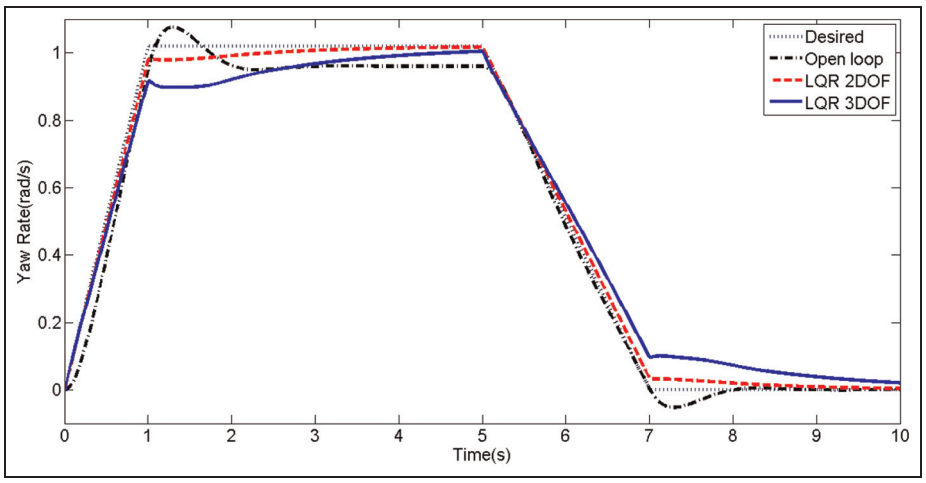

Figure 3. Yaw rate for a J-turn test with V = 30 m/s for various models.
LQR: linear quadratic regulator; 2DOF: two-degree-of-freedom; 3DOF: three-degree-of-freedom.

Controller design

In this section to design a robust LQR controller the LMI representation of this problem is presented; also the polytopic model of vehicle with simultaneous uncertainties in the cornering stiffnesses of the tyres and the speed of the vehicle is derived.

LMI representation of the LQR problem

This section presents an advanced LMI representation of the LQR problem as a framework for designing a robust LQR controller. We consider the linear time-invariant multiple systems[17]

$$\begin{aligned} \dot{X} &= A_j X + B_j u, \quad j = 1, \ldots, N \\ y &= F_j X + H_j u \end{aligned} \tag{21}$$

where N is the total number of multiple systems. In this equation the number of states and the number of inputs are n and p respectively. In the LQR problem, the cost function and the stability constraint with a state feedback control law $u = -KX$ are defined as[18]

$$J = \int_{t=0}^{t=\infty} (X^{\mathrm{T}} Q X + u^{\mathrm{T}} R u)\, \mathrm{d}t \tag{22}$$

$$\begin{aligned} J^* &= \min(J) \\ (A_j - B_j K)^{\mathrm{T}} P + P(A_j - B_j K) + Q + K^{\mathrm{T}} R K &< 0 \\ P \in R^{n \times n} &> 0 \\ j &= 1, \ldots, N \end{aligned} \tag{23}$$

In equation (23), P is the Lyapunov matrix which should be positive definite. Also K, Q and R are the controller gain, the weight matrix for the states and the weight matrix for the inputs respectively. When the state feedback control action $u = -KX$ is substituted in equation (22), this gives

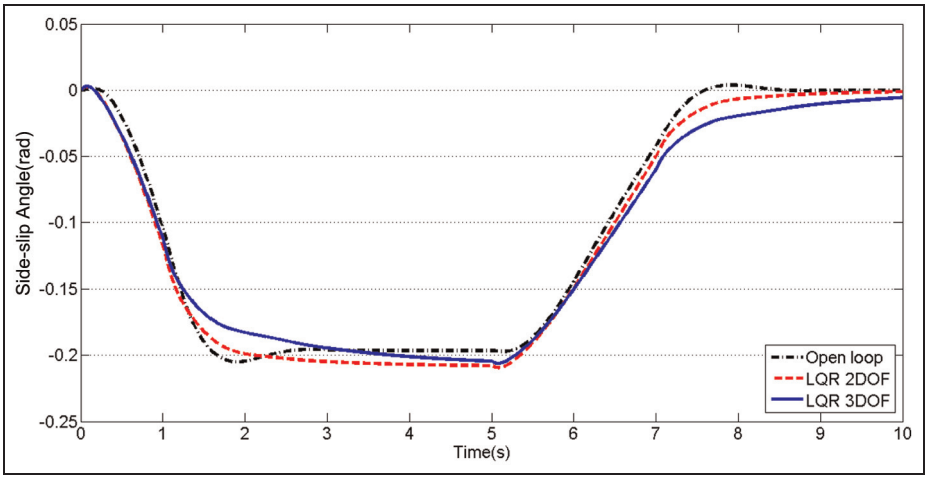

Figure 4. Side-slip angle for a J-turn test with V = 30 m/s for various models.
LQR: linear quadratic regulator; 2DOF: two-degree-of-freedom; 3DOF: three-degree-of-freedom.

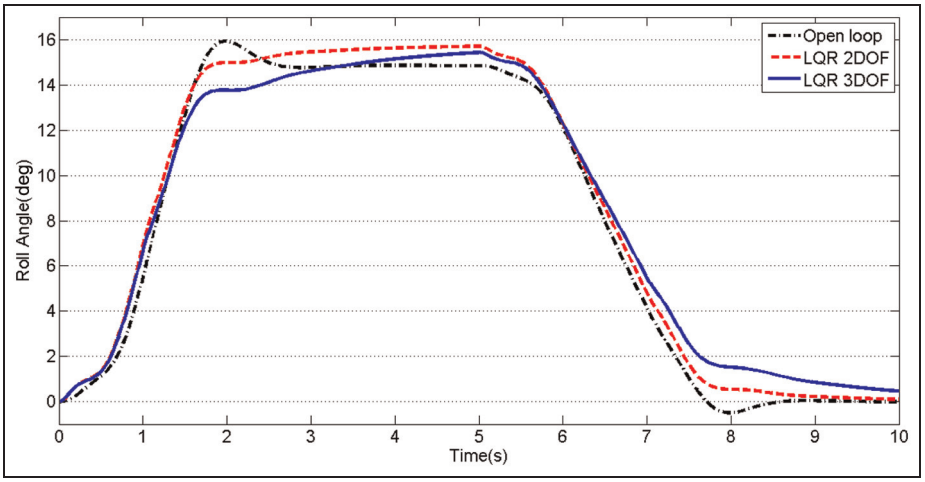

Figure 5. Roll angle for a J-turn test with V = 30 m/s for various models.
LQR: linear quadratic regulator; 2DOF: two-degree-of-freedom; 3DOF: three-degree-of-freedom.

$$J = \int_0^\infty \left[X^{\mathrm{T}}(Q + K^{\mathrm{T}}RK)X\right] \mathrm{d}t \tag{24}$$

Using the trace operator, equation (24) can be expressed as[11]

$$\begin{aligned} J &= \int_0^\infty \mathrm{Tr}\left[(Q + K^{\mathrm{T}}RK)XX^{\mathrm{T}}\right] \mathrm{d}t \\ &= \mathrm{Tr}\left[(Q + K^{\mathrm{T}}RK)Y\right] \\ Y &= \int_0^\infty (XX^{\mathrm{T}}) \mathrm{d}t \end{aligned} \tag{25}$$

Because of the linearity of the trace operator, equation (25) can be represented as

$$\begin{aligned} J &= \mathrm{Tr}(QY) + \mathrm{Tr}\left[R^{1/2}KYK^{\mathrm{T}}(R^{1/2})^{\mathrm{T}}\right] \\ J^* &= \min_{(K,\,Y)}\left\{\mathrm{Tr}(QY) + \mathrm{Tr}\left[R^{1/2}KYK^{\mathrm{T}}(R^{1/2})^{\mathrm{T}}\right]\right\} \end{aligned} \tag{26}$$

Note that the existence of the KY term in equation (26) changes its nature to a non-linear form. Hence, a change in the variable is used to solve this problem as[18]

$$\hat{X} > R^{1/2}KYK^{\mathrm{T}}(R^{1/2})^{\mathrm{T}} \tag{27}$$

The new variable $\hat{X}$ is an upper bound for the non-linear term in equation (26) and, with this change in the variable, the optimal magnitude of the cost function is defined as

$$J^* = \min\left[\mathrm{Tr}(QY) + \mathrm{Tr}(\hat{X})\right] \tag{28}$$

The presence of the KY term in equation (27) makes this constraint non-linear. To present this non-linear constraint in the LMI form, the changes in the variables

$$\begin{aligned} &K = \Lambda Y^{-1}, \quad K \in R^{p\times n}, \quad \Lambda \in R^{p\times n} \\ &P = Y^{-1} \\ &Y > 0 \end{aligned} \tag{29}$$

should be made.[11,12] Note that in equation (29) the constraint $Y>0$ is added to guarantee that the$P$ matrix has positive definiteness. Using equation (29) and Schur's complement, equation (27) can be presented in the LMI form as

$$\begin{bmatrix} \hat{X} & R^{1/2}\Lambda \\ \Lambda^T R^{1/2} & Y \end{bmatrix} > 0 \tag{30}$$

By using the same changes in the variables and Schur's complement, equation (23) is presented in the LMI format as

$$\begin{bmatrix} (A_j Y + Y^{\mathrm{T}} A_j^{\mathrm{T}} - B_j \Lambda - \Lambda^{\mathrm{T}} B_j^{\mathrm{T}}) & \Lambda^{\mathrm{T}} & Y^{\mathrm{T}} \\ \Lambda & -R^{-1} & 0 \\ & 0 & -Q^{-1} \end{bmatrix} < 0$$
$$Y>0 \tag{31}$$

Finally, the LMI representation of the LQR problem can be presented as the cost function (28) with the constraints in equations (30) and (31). In the next part of this section, polytopic modelling of uncertain vehicle dynamics is presented.

Polytopic modelling of two-degree-of-freedom uncertain vehicle dynamics

Previous studies indicate that linear vehicle models are sensitive to the system's parameters. The longitudinal velocity of the vehicle, the cornering stiffness or the uncertainty in the vehicle mass may significantly change the responses of the model. It is essential for the controller to have the ability to treat these uncertainties correctly. Therefore in this section the polytopic representation of the uncertain vehicle model is expressed.

As mentioned before, the uncertainties which are assumed in this paper are the time-varying longitudinal velocity of the vehicle and parametric uncertainty in the cornering stiffnesses of the front tyres and the rear tyres. In fact, the vehicle speed is a time-varying parameter; also the stiffnesses of the tyres are non-linear functions of the friction coefficient, the normal force, the side-slip and other parameters. Therefore, in this study, the tyre forces are modelled by linear and uncertain models.

Because of the presence of uncertain and time-varying parameters in the vehicle dynamics, the matrices A and Bdepend on these uncertain or time-varying terms. Hence equation (21) can be defined as a function of these parameters according to

$$\dot{X}(t) = A(p)X(t) + B(p)u(t) \tag{32}$$

In equation (32), p is the vector of the uncertain or time-varying parameters. This vector consists of n_p uncertain terms: $p = (p_1, p_2, \ldots, p_{n_p})$. Each uncertain parameter p_i is bounded between its minimum value $\underline{p_i}$ and its maximum value $\bar{p}_i$ according to

$$p_i \in [\underline{p}_i\ \bar{p}_i] \tag{33}$$

The acceptable values of the vector p are constrained in a polytope in the parameter space $\mathbb{R}^{n_p}$ with $N = 2^{n_p}$ vertices $\{v_1, v_2, \ldots, v_N\}$. It is assumed that the set $\Psi = \{\Psi_1, \Psi_2, \ldots, \Psi_N\}$ is the projection of the matrix $[A(p), B(p)]$ for each vertex v_i. Therefore, the elements of the set Ψ are the extreme of a convex polytope, which contains the images for all admissible values of$p$. If the matrix $[A(p), B(p)]$ depends linearly on p, then $[A(p), B(p)]$ will be a subset of the convex hull of the set $\Psi = \{\Psi_1, \Psi_2, \ldots, \Psi_N\}$ according to[11]

$$[A(p), B(p)] \in \mathrm{Co}\{\Psi_1, \Psi_2, \ldots, \Psi_N\} := \left\{ \sum_{i=1}^{N} \alpha_i \Psi_i,\ \ \alpha_i \geqslant 0,\ \ \sum_{i=1}^{N} \alpha_i = 1 \right\} \tag{34}$$

For more explanation of the polytopic modelling of uncertain systems see the papers by Boyd et al.[18] and Bernussou et al.[19] In fact, the set Ψ in this model is equivalent to multiple systems. Also the convex structure of the polytopic model of a system helps us to use the equations given in the previous section in controller design.

As mentioned before, the vehicle speed and the cornering stiffnesses of the tyres are the only sources of uncertainty in the present study. Consideration of these parameters as vehicle uncertainties makes the 2DOF vehicle model a non-linear model, and so changes in the variables as given by

$$\begin{aligned} p_1 &= \frac{C_{\alpha f}}{V_x}, \quad p_1 \in \left[\frac{C_{\alpha\, fmin}}{V_{xmax}}, \frac{C_{\alpha\, fmax}}{V_{xmin}}\right] \\ p_2 &= \frac{C_{\alpha r}}{V_x}, \quad p_2 \in \left[\frac{C_{\alpha\, rmin}}{V_{xmax}}, \frac{C_{\alpha\, rmax}}{V_{xmin}}\right] \\ p_3 &= \frac{C_{\alpha f}}{2}, \quad p_3 \in \left[\frac{C_{\alpha\, fmin}}{2}, \frac{C_{\alpha\, fmax}}{2}\right] \\ p_4 &= V_x, \qquad p_4 \in [V_{xmin}, V_{xmax}] \end{aligned} \tag{35}$$

Thus, for this problem, $n_p = 4$ and $N = 16$, and so the dynamic equations of the 2DOF vehicle model (equation (20)) can be represented by the polytopic model using equation (35) and the assumptions

$$\begin{aligned} &C_{\alpha_1} = C_{\alpha_3} = \frac{C_{\alpha f}}{2}, \quad C_{\alpha_2} = C_{\alpha_4} = \frac{C_{\alpha r}}{2} \\ &V_y = V_x\beta, \qquad V_x = \text{constant} \end{aligned} \tag{36}$$

The governing dynamics equations of the 2DOF vehicle can be represented by

$$\begin{bmatrix} \dot{V}_y \\ \dot{r} \end{bmatrix} = \begin{bmatrix} -\frac{p_1 + p_2}{m} & \frac{-p_1 L_f + p_2 L_r}{m} - p_4 \\ \frac{-L_f p_1 + L_r p_2}{I_{zz}} & -\frac{L_f^2 p_1 + L_r^2 p_2}{I_{zz}} \end{bmatrix} \begin{bmatrix} V_y \\ r \end{bmatrix} + \begin{bmatrix} \frac{p_3}{m} \\ \frac{L_f p_3}{m} \end{bmatrix} \delta \tag{37}$$

Equation (37) gives the system matrices A and B which linearly depend on the vector of the uncertain

parameters; hence a polytope with $N = 16$ vertices can be defined such that it contains all the possible values of the uncertain matrices of the system.

Since the vehicle dynamics model does not have an integral state, in tracking applications a zero steady-state error cannot be guaranteed. The auxiliary state $\zeta(t)$is added to the system dynamics to provide an integral action which guarantees zero steady-state error. This state is the integral of the tracking error. In this study, the goal of the controller is to track the desired yaw rate, so that the augmented system dynamics which are used in the controller design are defined as

$$\begin{aligned}
\zeta(t) &= \int_0^{\infty} [r(t) - y(t)]\, \mathrm{d}t \\
\tilde{X} &= \begin{bmatrix} X \\ \zeta(t) \end{bmatrix} \rightarrow \dot{\tilde{X}} = \tilde{A}_j \tilde{X} + \tilde{B}_j u \\
\tilde{A}_j &= \begin{bmatrix} A_j & 0 \\ -C_j & 0 \end{bmatrix} \\
\tilde{B}_j &= \begin{bmatrix} B_j \\ -D_j \end{bmatrix} \\
C_j &= [0 \;\; 1] \\
D_j &= [0 \;\; 0] \\
j &= 1, .., 16
\end{aligned} \tag{38}$$

Finally by using the LMI representation of the LQR problem which is presented by equations (28), (31) and (32) and the polytopic modelling of the 2DOF vehicle dynamics in equations (37) and (38), the robust LQR controller can be designed. The CVX tool box which has been created in recent years[20] was used to solve this LMI problem.

Robust LQR controller performance

As mentioned before, in this section a robust LQR controller is designed on the basis of a 2DOF linear model of vehicle to improve its lateral stability, and the performance of the controller is studied using simulation results. The vehicle model which is used for simulation purposes is the 8DOF non-linear vehicle model. To clarify the advantages of the proposed controller versus the classic LQR controller, both a linear model and a non-linear model of the tyres are used in the 8DOF simulation model. The non-linear tyre model which is used in this paper is the well-known Pacejka non-linear tyre model.[21] Furthermore, the linear model is the linearized version of the non-linear Pacejka model; therefore these two different models have equivalent small side-slip angles. First, a robust LQR controller with the following specifications is designed.

The robustness of the designed controller to the stiffnesses of the front and rear tyres is 20%, and the robustness to the time-varying speed of the vehicle is 50%. The nominal velocity of the vehicle in designing the controller is assumed to be 20 m/s.

In order to illustrate the advantages of the presented controller, the results of the robust LQR controller are compared with the corresponding results of the classical LQR controller which is designed for the nominal vehicle parameters. The weight matrices which are used in controller design are

$$\begin{aligned}
Q &= \mathrm{diag}(100, 500, 500) \\
R &= \mathrm{diag}(10, 10)
\end{aligned} \tag{39}$$

Also the gain of the classical LQR controller and thegain of the robust LQR controller are

$$K_{robust} = \begin{bmatrix} 0.0899 & 4.8466 & -2.706 \\ 0.0899 & 4.8466 & -2.706 \end{bmatrix} \tag{40a}$$

and

$$K_{LQR} = \begin{bmatrix} 0.0051 & 2.1940 & -5 \\ 0.0051 & 2.1940 & -5 \end{bmatrix} \tag{40b}$$

respectively.

The controller gains are achieved using a trial-and-error procedure to find the solvable and best lateral stability performance for our vehicle model.

Simulation of the non-linear eight-degree-of-freedom model of vehicle with linear tyres

In this part, the non-linear 8DOF vehicle model with linear tyres is used as a simulation model. Two harmonic steering inputs with different longitudinal velocities (10 m/s and 30 m/s) are considered. In the first simulation the longitudinal velocity of the vehicle is assumed to be 10 m/s with –20% uncertainties in the stiffness of the front wheels and + 20% uncertainties in the stiffness of the rear wheels. In the second simulation vehicle the speed is 30 m/s and the other parameters are the same as for the first manoeuvre. All the results are shown in Figure 6. It should be noted that saturation of the actuator is considered in this study. Note that the dynamics of the actuators are not considered in this study, and the saturation is caused by mechanical limitation of the steering angle.

The results obtained indicate the improved performance of the presented robust LQR controller in comparison with that of the LQR controller. In Figure 6(a) and (b), the better performance of the robust LQR controller in tracking the desired yaw rate is shown. For example, in Figure 6(b), the robust LQR controller is an ideal tracker but the LQR controller has a 10% steady-state error. The control action signals, which are presented in Figure 6(e) and (f), show that the signal of the robust LQR controller is smaller than the corresponding signal of the LQR controller. Even in Figure 6(f) the controller action signal was saturated owing to mechanical limitation of the the steering angle of the wheels. Because of Figure 6(c) and (d), the side-slip angle of the vehicle for both controllers is stable.

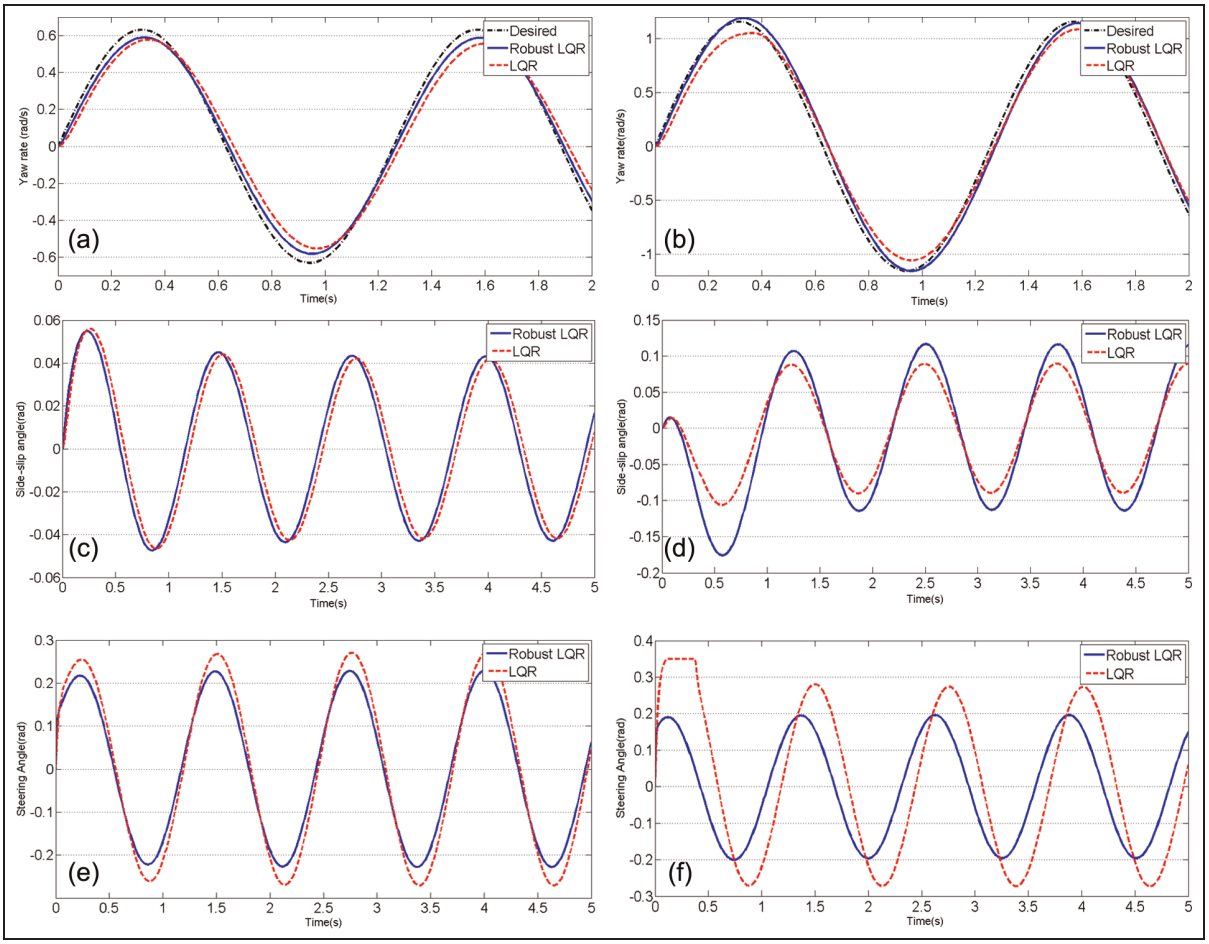

Figure 6. Comparison between the performances of the two controllers (the LQR controller and the robust LQR controller) at two different vehicle speeds and in the presence of uncertainties for a linear tyre model: (a) yaw rate tracking, V = 10 m/s; (b) yaw rate tracking, V = 30 m/s; (c) side-slip angle, V = 10 m/s; (d) side-slip angle, V = 30 m/s; (e) control action, V = 10 m/s; (f) control action, V = 30 m/s.
LQR: linear quadratic regulator.

Another important advantage of the presented robust LQR controller is the guaranteed stability of the uncertain system by the simple state feedback controller. In fact, it is possible to have an unstable closed-loop system when the LQR controller is used for a parameter-varying or uncertain system.

Another important property of this controller is its feasibility for real-time application, because the controller gain computation is performed offline and the structure of the controller is a state feedback type; hence this simple state feedback controller can guarantee the closed-loop stability of an actual vehicle in the presence of a large magnitude of the uncertainties and the time-varying speed.

In the next part of this section, the performance of the proposed controller in the presence of non-linearity of the wheels is studied.

Simulation of the non-linear eight-degree-of-freedom model of a vehicle with non-linear Pacejka tyres

In this section, the performance of the controller on a vehicle with non-linear tyres is studied. The cornering force is a non-linear function of the side-slip angle and also has saturation. Therefore, it could show the advantages of the proposed controller better than the linear tyre model does. In this section a harmonic steering input and also a J-turn manoeuvre are studied. In both cases, the longitudinal velocity of the vehicle is 30 m/s, and the magnitude and shape of the steering input are exactly the same as in the previous section. Figure 7(a) and (b) shows the yaw rate and the side-slip angle respectively in a harmonic manoeuvre. These parameters in the J-turn manoeuvre are indicated in Figure 7(c) and (d).

As shown in Figure 7(a) and (c), the performance of the robust LQR controller is clearly better than the corresponding performances of the LQR controller and of the open-loop system. Also, it can be seen that the LQR controller, which is designed for a nominal linear system, could not improve the yaw rate tracking performance and that the open-loop system has a better response. Moreover, the presence of an overshoot and an undershoot in Figure 7(c) are due to the high non-linearity of the non-linear Pacejka model; in fact, the uncertainty in the tyres is more than an

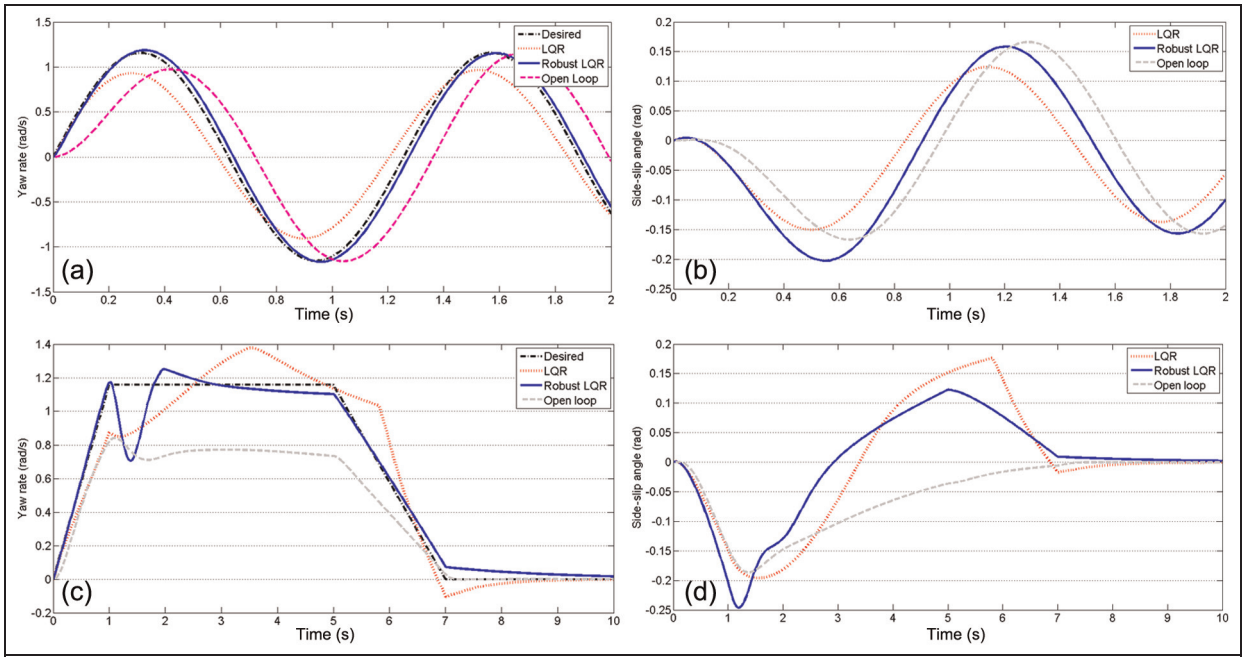

Figure 7. Comparison between the performances of the two controllers (the LQR controller and the robust LQR controller) at two different vehicle speeds and in the presence of uncertainties for a non-linear tyre model: (a) yaw rate, V = 30 m/s, harmonic input; (b) side-slip angle, V = 30 m/s, harmonic input; (c) yaw rate, V = 30 m/s, J-turn; (d) side-slip angle, V = 30 m/s, J-turn.

over-assumption in the robust controller design. However, the proposed controller can handle the non-linearity of the tyre models and shows its benefits and advantages in these simulations.

Figure 7(b) and (d) shows the lateral stability of the vehicle in these simulations.

Conclusions

In this paper a robust LQR active steering controller was designed on the basis of an LMI and polytopic modelling of the vehicle dynamics. This controller has good robustness due to the simultaneous presence of significant uncertainties in the longitudinal velocity of the vehicle and also the cornering stiffnesses of the tyres; also this controller is very simple to implement on an actual vehicle. Because the main difficulty of this controller is its calculation, and this part is carried out offline, thus the controller has the structure of a state feedback controller and can be implemented simply. The designed controller improves the lateral stability of the vehicle in the presence of 50% variation in the longitudinal velocity of the vehicle and 20% uncertainty in the cornering stiffnesses of the tyres. Also the effect of considering the roll dynamics in designing an active steering controller was studied. These investigations show that active steering can be used for vehicle roll control only at low speeds such as 10 m/s and that the roll dynamics effect is negligible in active steering controller design. In addition, simulations of the harmonic input and the J-turn results indicate that the robust LQR controller has a better performance than the LQR controller does.

Funding

This research received no specific grant from any funding agency in the public, commercial or not-for-profit sectors.

Declaration of conflict of interest

The authors declare that there is no conflict of interest.

References

1. Ackermann J, Odenthal D and Bunte T. Advantages of active steering for vehicle dynamics control. In: *32nd international symposium on automotive technology and automation*, Vienna, Austria, 14–18 June 1999, pp. 263–270. Croydon, Surrey: Automotive Automation Ltd.
2. Palkovics L, Semsey A and Gerum E. Rollover prevention system for commercial vehicles –additional sensor less function of the electronic brake system. *J Veh System Dynamics* 1999; 32: 285–297.
3. Chen E and Peng H. Differential-braking-based rollover prevention for sport utility vehicles with human-in-the loop evaluations. *J Veh System Dynamics* 2001; 36(4–5): 359–389.
4. Shim T, Toomey D, Ghike C et al. Vehicle rollover recovery using active steering/wheel torque control. *Int J Veh Des* 2008; 46(1): 51–71.
5. Falcone P, Borrelli F, Tseng HE et al. Linear time-varying model predictive control and its application to active steering systems: stability analysis and

experimental validation. *Int J Robust Nonlinear Control* 2008; 18: 862–875.
6. Zhang JY, Kim JW, Lee KB et al. Development of an active front steering (AFS) system with QFT control. *Int J Automot Technol* 2008; 9(6): 695−702.
7. Hsu Y-H J and Gerdes JC. Stabilization of steer-by-wire vehicle at the limits of handling using feedback linearization. In: *ASME international mechanical engineering congress and exposition, Dynamic systems and control*, Parts A and B, Orlando, Florida, USA, 5–11 November 2005, paper IMECE2005-81203, pp. 483–492. New York: ASME.
8. Baslamisli SÇ, Köse IE and Anlaş G. Gain-scheduled integrated active steering and differential control for vehicle handling improvement. *J Veh System Dynamics* 2009; 47(1): 99–119.
9. Minoiu Enache N, Netto M, Mammar S et al. Driver steering assistance for lane departure avoidance. *J Control Engng Practice* 2009; 17: 642–651.
10. Goodarzi A, Rahiminejad D and Esmailzadeh E. Design of a fuzzy controller for independent control of front wheels steering angle. In: *ASME international design engineering technical conference, 11th international conference on advanced vehicle and tire technologies*, San Diego, California, USA, 30 August–2 September 2009, Vol 6, paper DETC2009-87748, pp. 1061–1067. New York: ASME.
11. Olalla C, Leyva R, El Aroudi A et al. Robust LQR control for PWM converters: an LMI approach. *IEEE Trans Ind Electron* 2009; 56(7): 2548–2558.
12. Ko HS, Jatskevich J, Dumont G et al. An advanced LMI-based-LQR design for voltage control of grid-connected wind farm. *J Electric Power Systems Res* 2008; 78: 539–546.
13. He J, Crolla DA, Levesley MC and Manning WJ. Coordination of active steering, driveline, and braking for integrated vehicle dynamics control. *Proc IMechE Part D: J Automobile Engineering* 2006; 220(10): 1401–1420.
14. Rajamani R. *Vehicle dynamics and control*. Berlin: Springer, 2001.
15. Jazar RN. *Vehicle dynamics: theory and application*. Berlin: Springer, 2009.
16. Howe JG, Garrott WR and Forkenbrock GJ. An experimental examination of selected maneuvers that may induce on-road, untripped light vehicle rollover – phase I-A of NHTSA's 1997–1998 Light Vehicle Rollover Research Program. NHTSA Technical Report DOT HS 809 357, National Highway Traffic Safety Administration, Department of Transportation, Washington, DC, USA, August 2001.
17. Anderson BDO and Moore JB. *Optimal control: linear quadratic methods*. Englewood Cliffs, New Jersey: Prentice-Hall, 1998.
18. Boyd S, El Ghaoui L, Feron E et al. *Linear matrix inequalities in system and control theory*, SIAM Studies in Applied Mathematics, Vol 15. Philadelphia, Pennsylvania: SIAM, 1994.
19. Bernussou J, Peres PLD and Geromel J. A linear programming oriented procedure for quadratic stabilization of uncertain systems. *J Systems Control Lett* 1989; 13(1): 65–72.
20. Grant M and Boyd S. CVX: Matlab software for disciplined convex programming, version 1.21/cvx, http://cvxr.com/cvx (April 2011).
21. Pacejka HB, Bakker E and Lidner L. A new tire model with an application in vehicle dynamics studies. SAE paper 890087, 1989.

Appendix I

Terms used in the three-degree-of-freedom linear model of the vehicle (equation (19))

The terms used in equation (19) are

$$
\begin{aligned}
G_{11} &= -A_{11}(C_{\alpha_1}+C_{\alpha_2}+C_{\alpha_3}+C_{\alpha_4})\\
G_{12} &= -\frac{C_{\alpha_1}L_fA_{11}}{V_x}-\frac{C_{\alpha_3}L_fA_{11}}{V_x}+\frac{C_{\alpha_2}L_rA_{11}}{V_x}\\
&\quad+\frac{C_{\alpha_4}L_rA_{11}}{V_x}+A_{13}\\
G_{13} &= -K_{\varphi f}A_{12}-K_{\varphi r}A_{12}\\
G_{14} &= -A_{12}C_{\varphi f}-A_{12}C_{\varphi r}\\
G_{21} &= \frac{-C_{\alpha_1}L_f-C_{\alpha_3}L_f+C_{\alpha_2}L_r+C_{\alpha_4}L_r}{I_{zz}}\\
G_{22} &= \frac{-C_{\alpha_1}L_f^2-C_{\alpha_3}L_f^2-C_{\alpha_2}L_r^2+C_{\alpha_4}L_r^2}{I_{zz}V_x}\\
G_{41} &= -B_{12}(C_{\alpha_1}+C_{\alpha_2}+C_{\alpha_3}+C_{\alpha 4})\\
G_{42} &= B_{13}-\frac{B_{12}C_{\alpha_1}L_f}{V_x}-\frac{B_{12}C_{\alpha_3}L_f}{V_x}+\frac{B_{12}C_{\alpha_2}L_r}{V_x}\\
&\quad+\frac{B_{12}C_{\alpha_4}L_r}{V_x}\\
G_{43} &= -K_{\varphi f}B_{11}-K_{\varphi r}B_{11}\\
G_{44} &= -C_{\varphi f}B_{11}-C_{\varphi r}B_{11}\\
A_{11} &= a_{11}+a_{16}\\
A_{12} &= a_{12}\\
A_{13} &= a_{13}+a_{14}+a_{15}\\
B_{11} &= \frac{1+A_{12}m_sh}{I_{xxs}+m_sh^2}\\
B_{12} &= \frac{A_{11}m_sh}{I_{xxs}+m_sh^2}\\
B_{13} &= \frac{A_{13}+m_shu}{I_{xxs}+m_sh^2}\\
a_{11} &= \frac{I_{xxs}}{mI_{xxs}+mm_sh^2-m_s^2h^2}\\
a_{12} &= \frac{m_sh}{mI_{xxs}+mm_sh^2-m_s^2h^2}\\
a_{13} &= \frac{m_s^2h^2u}{mI_{xxs}+mm_sh^2-m_s^2h^2}\\
a_{14} &= -\frac{muI_{xxs}}{mI_{xxs}+mm_sh^2-m_s^2h^2}\\
a_{15} &= -\frac{mm_sI_{xxs}h^2}{mI_{xxs}+mm_sh^2-m_s^2h^2}\\
a_{16} &= \frac{m_sh^2}{mI_{xxs}+mm_sh^2-m_s^2h^2}
\end{aligned}
$$

Appendix 2

The parameters for the SUV are given in Table 4.

Table 4 Parameters for the SUV.

Parameter symbol and value	Definition of the parameter
$I_{zz} = 2000$ kg m^2	Yaw moment of inertia
$I_{xxs} = 900$ kg m^2	Roll moment of inertia
$m_s = 1440$ kg	Sprung mass
$m_{uf} = 40$ kg	Front unsprung mass
$m_{ur} = 40$ kg	Rear unsprung mass
$L_f = 1.016$ m	Distance from the centre of gravity to the front axle
$L_r = 1.524$ m	Distance from the centre of gravity to the rear axle
$K_{\varphi f} = 30,000$ Nm/rad	Stiffness of the front suspension
$K_{\varphi r} = 20,000$ Nm/rad	Stiffness of the rear suspension
$C_{\varphi f} = 1897$ Nm/rads	Damping coefficient of the front suspension
$C_{\varphi r} = 1265$ Nm/rads	Damping coefficient of the rear suspension
$T = 1.5$ m	Width of the track
$R = 0.334$ m	Radius of the wheel
$I_w = 1.2$ kgm^2	Moment of inertia of the wheel
$h = 0.75$ m	Height of the centre of gravity
$C_{\alpha f} = 57,296$ N/rad	Cornering stiffness of the front axle
$C_{\alpha r} = 52,712$ N/rad	Cornering stiffness of the rear axle
$C_{\alpha i}$ (N/rad)	Cornering stiffness of the *i*th tyre
V_x (m/s)	Longitudinal speed of the vehicle
V_y (m/s)	Lateral speed of the vehicle
β (rad)	Centre-of-mass side-slip angle of the vehicle
r (rad/s)	Yaw rate of the vehicle
φ (deg)	Roll angle of the vehicle